JJEE

Volume 12 | Number 1 | March 2026 | Pages 112-123

Jordan Journal of Electrical Engineering

ISSN (print): 2409-9600, ISSN (online): 2409-9619

Homepage: jjee.ttu.edu.jo

Automatic Detection and Recognition for Linear Frequency Modulated SAR Signals in a Compact Radiomonitoring Module

The Quan Trong[1], Nguyen Trong Nhan[2*]

[1] Faculty of Information Security, Posts and Telecommunications Institute of Technology, Hanoi, Vietnam
[2] Department of Radar Research, Air Defence-Air Force Technical Institute, Hanoi, Vietnam
E-mail: 10th20th30th@gmail.com

Received: Sep 17, 2025 *Revised: Dec 02, 2025* *Accepted: Dec 22, 2025X* *Available online: Mar 19, 2026*

***Abstract*—** This paper presents a complete algorithmic framework for the automatic detection, parameter estimation, and recognition of Linear Frequency Modulated (LFM) synthetic aperture radar (SAR) signals within a compact radiomonitoring module. The proposed method integrates a parallel frequency-based search, an autocorrelation-based detection stage, time–frequency parameter extraction, and a Bayesian decision scheme for signal classification. A key feature of the approach is its implementation within an autocorrelation-type receiver, which enables precise estimation of LFM parameters at low signal-to-noise ratios while maintaining the small size, low weight, and low power consumption required for deployment on both stationary and mobile platforms. The simulation results indicate that the parameter estimation error does not exceed 8%, and the classification probability approaches unity for representative SAR signal types at signal-to-noise ratios above 0 dB. These results confirm the effectiveness of the proposed algorithm for compact radiomonitoring applications.

***Keywords*—** Automatic processing; Autocorrelation receiver; Synthetic aperture radar; LFM signal.

1. INTRODUCTION

Modern synthetic aperture radar (SAR) systems are among the most advanced tools in contemporary radar technology. Their information capacity is enhanced through the use of various ground observation modes (stripmap, spotlight, scan, etc.) and operating modes (polarimetric, interferometric, etc.), which generally require two or more channels for trajectory signal processing. Current SAR systems are capable of generating high-resolution radar images (with resolutions ranging from 0.1 to 5 m) using various types of aerial platforms [1-3]. Since SAR employs complex signals, such as linear frequency modulated (LFM) waveforms, specialized algorithms for signal reception and processing are required in radiomonitoring systems. Given the a priori uncertainty of LFM signal parameters, their processing can be effectively implemented using an autocorrelation receiver (ACR) [4-7].

Moreover, many radiomonitoring systems lack compact devices capable of detecting radar illumination of various objects by airborne or space-based systems. The use of standard radiomonitoring complexes for this purpose is impractical for stationary deployment and impossible in mobile scenarios [8-10]. Therefore, it is necessary to develop a compact receiving device that can determine the parameters of LFM signals. Such a device should be installed directly on or within objects and infrastructure, providing real-time warnings of SAR illumination and delivering information on the resolution of radar images generated by SAR. Previous studies have examined the feasibility of using autocorrelation processing for

* Corresponding author
DOI: https://doi.org/10.5455/jjee.204-1758123818

modulation recognition [4], evaluated computational complexity aspects of such receivers [5], and analyzed the accuracy of localization when processing complex and broadband signals [6]. Further research demonstrated that autocorrelation receivers offer robust detection characteristics for both simple radio pulses and signals with LFM or PSK modulation, even under low-SNR conditions [7]. More recent work has also confirmed their suitability for compact radiomonitoring modules, highlighting the potential for reduced hardware complexity and improved noise immunity [8-11].

Despite these contributions, existing literature primarily focuses on individual components—modulation identification, complexity analysis, or detection performance—without addressing a unified and fully automatic processing chain suitable for recognizing SAR-LFM signals. This gap is especially significant because practical radiomonitoring applications require not only detection but also precise parameter estimation and classification of LFM radar emissions operating in dense electromagnetic environments.

To address this need, the present work proposes a complete end-to-end algorithm integrating frequency search, autocorrelation-based detection, time–frequency parameter estimation, and Bayesian classification, specifically optimized for implementation in compact radiomonitoring modules.

The aim of this paper is to develop an algorithm for the automatic processing of LFM signals in a compact radiomonitoring module.

2. TECHNICAL JUSTIFICATION OF AN AUTOCORRELATION RECEIVER FOR SAR SIGNALS

The requirements for an ACR should be formulated based on the evaluation of the radiomonitoring system efficiency. In turn, the efficiency of such a system may be assessed according to different criteria and expressed in various units, depending on the end users it serves.

The main technical characteristics of the autocorrelation receiver for SAR signals in the X-, L-, and C-bands are as follows: Type of received signal – pulsed LFM; RF bandwidth (pulse duration) Δf_{HF} (τ_p); Frequency modulation rate (delay duration) v_f (τ_d); IF bandwidth Δf_{LF}; Receiver sensitivity $P_{\min}$; Antenna gain G_{m}; Detection range D_{m}; Antenna beamwidth θ_{a}; Number of receiving channels by direction *N*; Number of receiving channels by frequency *M*.

Figure 1 illustrates the ACR structure used in this study, adopted from established literature [4–7], and integrated into the proposed processing chain. The diagram of the proposed ACR (Fig. 1) includes: high-pass band-pass filter (BF HF) with a passband Δf_{HF}; delay line DL with delay duration τ_d; multiplier; low-pass filter (LF) with a passband Δf_{LF}; parameter measurement block (PMB).

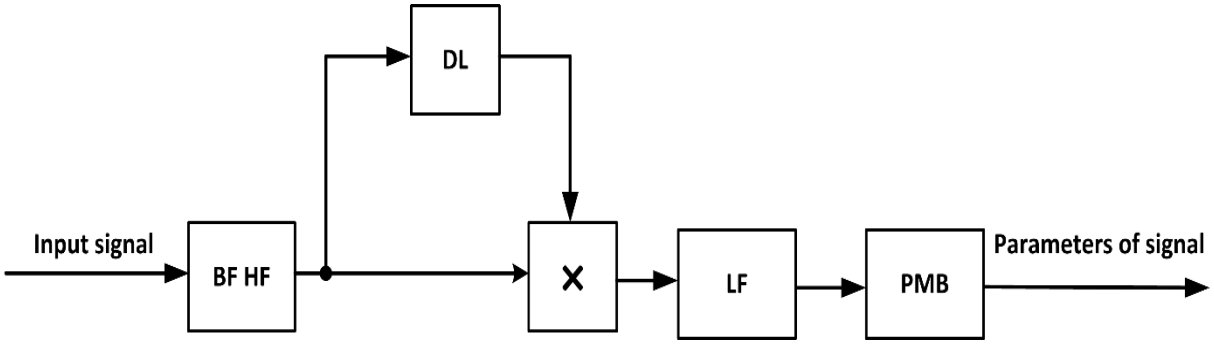

Fig. 1. Block diagram of an autocorrelation receiver.

The operating principle of the ACR is based on extracting the low-frequency component at the difference frequency after multiplying the received signal by its delayed copy, which enables recognition of the LFM signal and determination of its parameters. Let us consider the mathematical model of LFM signal processing in the ACR. The block diagram of this model is shown in Fig. 2. While the general principles of autocorrelation processing have been examined in previous works [4–7], all computer simulations presented in this paper were carried out by the authors using the mathematical model adapted for the proposed processing algorithm. For the purpose of defining the limitations and assumptions in justifying the ACR scheme, the following technical specifications are adopted: High-frequency bandpass filter bandwidth: $\Delta f_{HF} = 80$ MHz or 500 MHz; Low-frequency bandpass filter bandwidth: $\Delta f_{HF} = 5$ MHz (for X-band signals), $\Delta f_{HF} = 2$ MHz (for C-band signals). The probing signals are listed in Table 1.

Table 1. LFM Signal parameters.

№ signal	Parameters				
	f_s[GHz]	Δf_s [MHz]	τ_p [μs]	v_f [MHz/μs]	*SNR* [dB]
1	9.65	400	80	5	-15…5
2	9.65	138	40	3.45	-15…5
3	5.35	225	20	11.25	-15…5
4	5.35	18.75	20	0.94	-15…5

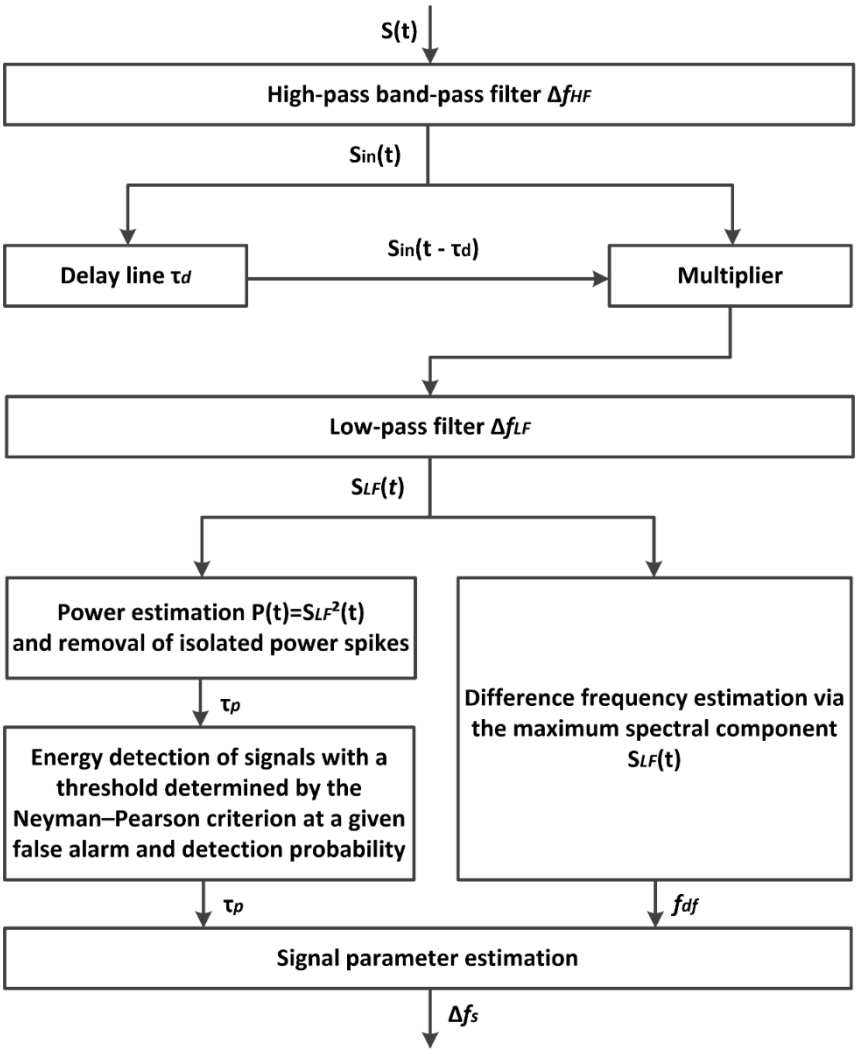

Fig. 2. Block diagram of the mathematical model of LFM signal processing in the ACR.

Simulation of the processing of probing LFM SAR signals in the ACR showed the following results: For X-band probing signals, under the specified initial conditions, the error in determining the signal spectrum width did not exceed 2.5%, with the maximum error occurring at the minimum v_f = 1 MHz/μs; For C-band probing signals, under the specified initial conditions, the error in determining the signal spectrum width did not exceed 3%, except in the case of simulating an LFM signal with a v_f = 0.94 MHz/μs, where the maximum error reached 7.61%.

It should be noted that, prior to developing the processing algorithm, we calculated the expected detection range D_m of airborne and spaceborne SAR signals when using an autocorrelation receiver (ACR). These calculations were carried out to determine the minimum antenna gain required for reliable reception, assuming a receiver sensitivity of $P_{min} \geq -120$ dB Using the detection-range estimation methodology described in [11], the results showed that, at typical operational ranges and considering both main-lobe and side-lobe illumination, a radiomonitoring system requires an antenna gain of at least $G_m \geq 2$ to ensure stable detection of SAR signals.

To enable efficient detection of wideband synthetic-aperture radar (SAR) emissions, the proposed processing chain employs a parallel directional frequency search strategy. This approach performs simultaneous energy probing across multiple narrow angular–frequency sectors, which significantly accelerates the search stage compared with traditional sequential scanning. The beamwidth of the radiomonitoring antenna is estimated using the well-established approximation:

$$\theta_{\mathrm{a}[rad]} = \sqrt{\frac{k4\pi^2}{G_{\mathrm{m}}}},\ k \in [0.4,0.8] \tag{1}$$

where G_{m} denotes the antenna gain and k is the illumination-dependent coefficient determined by the aperture distribution [12, 13]. Eq. (1) provides the fundamental angular resolution that constrains how many parallel beams may be formed without mutual overlap. For omnidirectional radiomonitoring, the required number of channels is:

$$N = \frac{360^0}{\theta_{a[rad]}} \tag{2}$$

From Eqs. (1) and (2), the antenna beamwidth and corresponding scanning step directly determine the number of parallel directional branches required for full coverage of the monitored angular sector. For the operational parameters considered in this study, these equations yield a minimum of $N = 6$ parallel search channels. This configuration, illustrated in Fig. 3, ensures that the entire surveillance region is simultaneously probed with no angular gaps, thereby enabling reliable detection of short-duration SAR signals under low-SNR conditions.

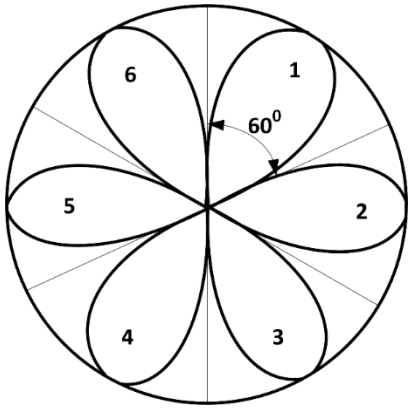

Fig. 3. Radiation pattern of the directional search antenna in ACR operation.

In radiomonitoring stations, each spatial channel is associated with its own receiving channel [14-16]. Direction finding in such a station is performed according to the number of the receiver channel in which the radar signal is detected.

If the radar signal is received not by a single but by several adjacent antenna pattern lobes, further refinement of the direction can be achieved by comparing the amplitudes or phases of the received signals in these adjacent channels.

With this approach, direction finding of the radar is performed almost without time delays, and the reception duration corresponds to the illumination time of the radiomonitoring station.

In the ACR, frequency search represents the process of systematically scanning a specific portion of the frequency band $\Delta f = f_{max} - f_{min}$ (Fig. 4) by sequentially turning the radiomonitoring receiver, which has a finite bandwidth Δf_{HF}. Similar to directional search, it constitutes one of the methods for conducting radiomonitoring.

The ultimate result of frequency search within the L, C, X1, and X2 bands is the detection of signals from active radio-emission sources (Fig. 5) [17, 18].

The number of frequency channels is defined as:

$$M = \frac{\sum_i \Delta f_i}{\Delta f_{HF}} \quad (3)$$

where Δf_i – the bandwidth of the i-th operating frequency range of the SAR; i – the index of the operating frequency range of the SAR. With Eq. (3), the required number of receiver switching operations for implementing sequential frequency search is calculated in Table 1.

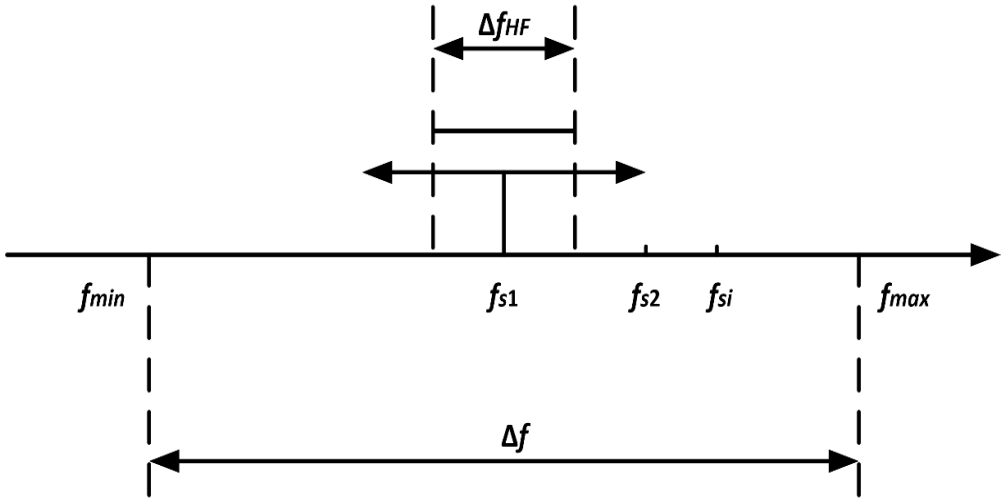

Fig. 4. Frequency search.

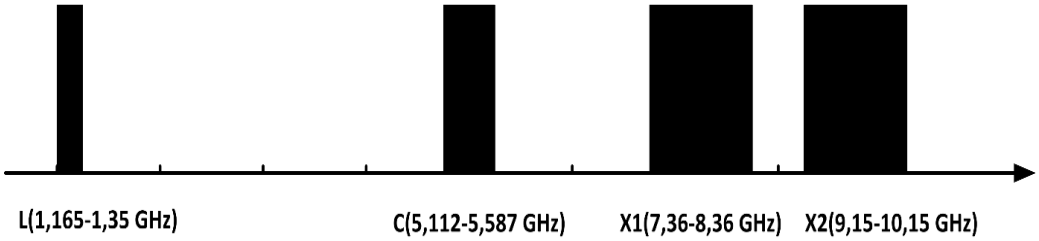

Fig. 5. L, C, X1, X2 frequency bands.

Based on the number of frequency channels (Table 2) and the maximum pulse repetition period of SARs with different configurations, the search time of SAR emissions by frequency can be calculated. Consequently, the total search time of SAR emissions by both direction and frequency can be determined.

Table 2. Required receiver switching operations for sequential frequency search.

Frequency range (carrier frequency, GHz)	L(1,2575)	C(5,35)	X1(7,86)	X2(9,65)	Total number of frequency search channels
Operating frequency range (MHz)	185	475	1000	1000	-
Number of frequency channels under the condition Δf_{HF} = 500 MHz	1	1	2	2	6
Number of frequency channels under the condition Δf_{HF} = 80 MHz	3	6	13	13	35

3. ALGORITHM DEVELOPMENT FOR SAR RECOGNITION USING TIME–FREQUENCY PARAMETERS OF LFM SIGNALS

The parameters of SAR signals and their variations serve as revealing intelligence features. Identifiable features are those that allow the detection of SAR radiation activity and the determination of its operational mode and type. These features comprise the technical parameters of SAR emissions and the manner in which the SAR is employed. The technical parameters are mainly characterized by the frequency and time properties of the probing signals.

The frequency-related parameters include the carrier frequency (f_s), the pulse repetition frequency (PRF_p), the burst repetition frequency (F_{br}), and, if applicable, the law of carrier frequency variation. The burst repetition frequency (F_{br}) is determined by the angular velocity of the SAR antenna scan and the size of the antenna beam scanning sector. This parameter characterizes the rate at which the SAR antenna beam intersects the field of view of the electronic surveillance system.

The time-related parameters of SAR signals include the pulse duration (τ_p), the pulse repetition interval (PRI_p), the burst duration (τ_{br}), the scan period (T_{scan}), and the law of burst envelope variation. The burst duration (τ_{br}) observed in electronic surveillance systems is determined by the antenna beamwidth and the angular scan rate of the SAR antenna in the horizontal plane. The law of envelope variation can indicate the presence or absence of spatial scanning by the SAR antenna.

To achieve the primary objective of SAR recognition, an informed decision must first be made regarding the set of features by which the system will identify SAR objects. It can be concluded that the most informative recognition features: f_s, Δf_s, PRF_p, PRI_p. It should also be noted that all SAR systems are characterized by a carrier frequency range; therefore, the pulse duration of the probing signals and other related parameters must be considered.

Based on Bayes' formula, an algorithmic scheme (Fig. 6) was developed for SAR recognition using the time–frequency parameters of LFM signals. Although Bayesian decision theory is well established in signal recognition and has been extensively discussed in the literature [19, 20], the present work does not claim the Bayesian framework itself as a contribution. Instead, our contribution lies in adapting and integrating Bayesian inference into a specialized recognition scheme tailored for LFM-based SAR signals within a compact radiomonitoring module. In the proposed approach, Bayes' formula is reformulated for joint

use with the time–frequency features extracted by the autocorrelation receiver, enabling a unified multi-stage chain for detection, parameter estimation, and classification.

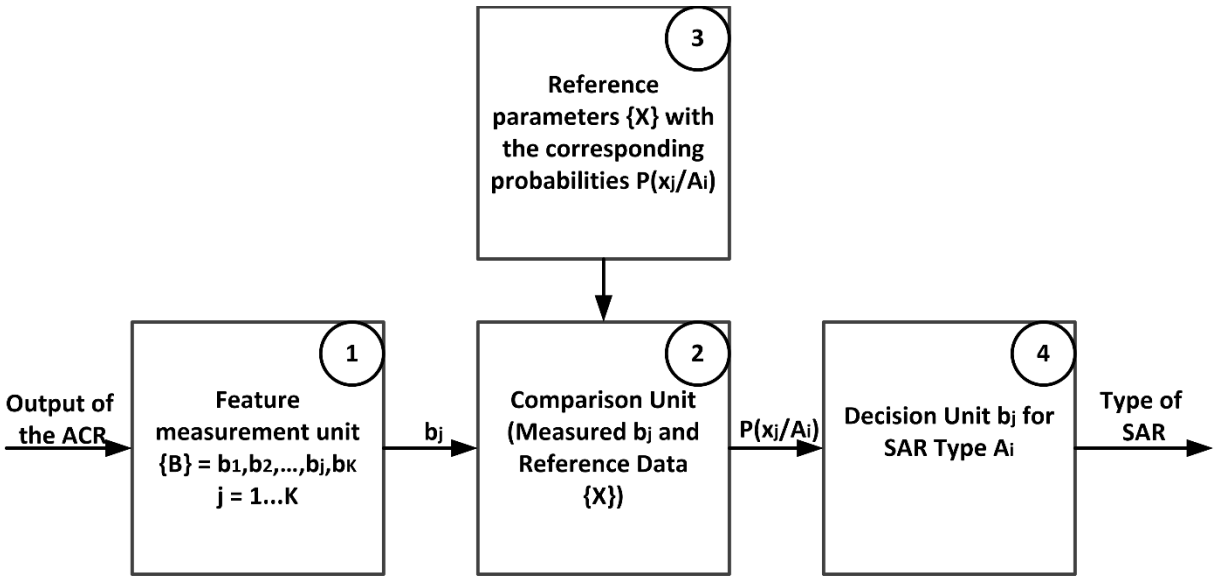

Fig. 6. Block diagram of the algorithm for SAR recognition based on the time–frequency parameters of LFM signals.

The signal from the electronic surveillance receiver is fed into Block 1, where its parameters are measured. Each measured parameter b_i is then forwarded to the comparison unit (Block 2), in which it is compared with the reference data stored in the memory unit (Block 3). Depending on the degree of correspondence between the measured parameters b_i and the reference data, the memory unit outputs to the decision-making device (Block 4) the conditional probability that the received signal with the measured parameters b_i belongs to a specific SAR type A_i. To assess the performance of the proposed SAR-signal classification algorithm, numerical simulations were conducted in MATLAB using the parameters defined in Subsection 2. Signals 1 and 2 correspond to COSMO-SkyMed-type SAR waveforms, while Signals 3 and 4 represent RISAT-1-type waveforms.

The results indicate that the simulation results validate that the proposed method achieves high classification accuracy in both low-SNR conditions. As the SNR increases from –15 dB to 5 dB, the probability of correct classification improves steadily: approximately by 3% for COSMO-SkyMed signals and by 9% for RISAT-1 signals. At SNR $\geqslant$ 0 dB, the probability of correct classification approaches unity for all evaluated SAR types, and the probability of misclassification becomes negligible. This behavior confirms that the proposed Bayesian-based decision rule effectively exploits the intrinsic characteristics of the signal parameters. Furthermore, the difference in classification gain between the two SAR families reflects their distinct modulation structures, which are captured reliably by the feature set used in the algorithm.

4. DEVELOPMENT OF AN OPERATING ALGORITHM FOR A COMPACT AUTOMATIC DEVICE FOR SAR SIGNAL MONITORING

The developed algorithms for determining the frequency–time parameters of SAR signals and their recognition, as well as the justification of the technical characteristics of the

compact radiomonitoring device, make it possible to proceed with the description of the overall operating process of the proposed system. The primary requirement for the operating algorithm of the compact radiomonitoring device is the capability to automatically process the received signals and provide output information to the end-user without operator intervention. The structural block diagram of the operating algorithm of the compact automatic SAR signal monitoring device is presented in Fig. 7. The operating principle of the developed device can be summarized as follows.

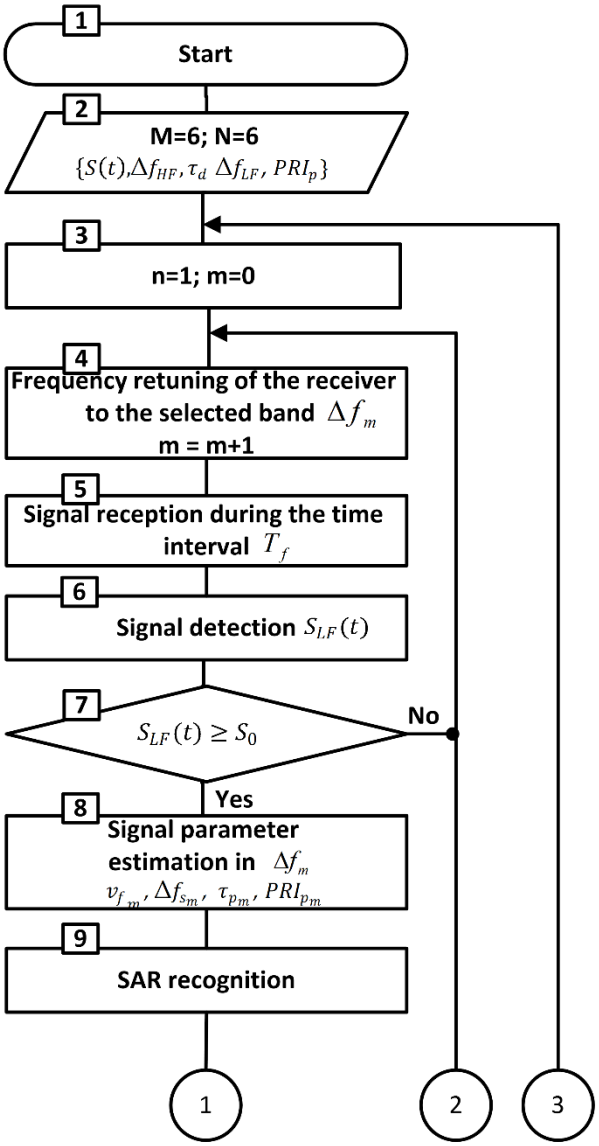

Fig. 7. Structural block diagram of the operating algorithm of the compact automatic SAR signal monitoring device (beginning).

After power-up and initialization of the device hardware, the following information is retrieved from the non-volatile memory (Block 2): the number of angular channels N = 6; the number of frequency channels M = 6; and data on the frequency–time parameters of SAR signals operating in different modes. The search for SAR probing signals then begins, carried out by direction (azimuth only, since the beamwidth of the radiomonitoring antenna ensures reception across all elevation angles) and within the ranges of their operational frequencies.

The receiver is connected to the first antenna (nominally) and tuned to the frequency band Δf_1 (Blocks 3 and 4). Within each frequency band, the probing signals must be received

for a sufficient duration to correctly determine the SAR pulse duration PRF_p. This observation time is denoted as T_f,which is defined as:

$$T_f = 2{,}5 * PRI_{p\,max} * M \quad (4)$$

where $PRI_{p\,max}$ – the maximum possible pulse repetition interval of the SAR probing signal.

The SAR probing signals enter the first channel of the receiving unit (n = 1, m = 1) (Block 4), which is tuned to the frequency band Δf_m. In Block 5, the timing of signal reception begins over the interval T_f. The received signal $S_{LF}(t)$ must exceed the detection threshold level S_0. In Block 6, the condition $S_{LF}(t) \geq S_0$ is verified. If the condition $S_{LF}(t) \geq S_0$ is not satisfied (no signal is present), the receiver switches to the next frequency search channel. If the condition $S_{LF}(t) \geq S_0$ is satisfied (signal detected), then in Block 8 the parameters of the signal received in the m-th frequency channel are determined: $v_{f\,m}$, Δf_{s_m}, τ_{p_m}, PRI_{p_m} (Fig. 2).

Based on the measured parameters of the probing signal, Block 9 performs recognition of the SAR platform type (satellite, aircraft, or UAV) (Fig. 8). These operations are repeated until the condition $m = M$ (all SAR operational frequency ranges scanned) is satisfied in Block 10. Once the frequency–time parameters of the probing signals are determined across all frequency channels, Block 11 computes the overall spectral width Δf_s using identical values of v_f, τ_p, PRI_p. Block 11 may also refine the estimates of the pulse duration τ_p and pulse repetition interval PRI_p by excluding anomalous measurements and applying averaging with current estimates. Subsequently, in Block 12, the antenna is switched by azimuth angle β_n, where the above operations are repeated for each frequency channel m. After the condition $n = N$ is satisfied, azimuthal scanning is considered complete (Block 13).

All frequency–time parameters of the probing signal determined in the n-th channel are sent to Block 14, where, first, the aperture synthesis time of the SAR of T_{SAR} is calculated, which may last several tens of seconds; second, the imaging range of the formed radar images is computed, with range and azimuth resolution). After these calculations, the results of radiomonitoring are stored in memory and displayed to the user (Block 15). In parallel with outputting the information to the operator, the device is switched back to the initial spatial and frequency channels. All the above procedures are subsequently executed automatically, without operator intervention, until the power supply is turned off.

Considering Eq. (4), the total scanning time of the receiver T_{scan} is defined as:

$$T_{scan} = T_f * \mathrm{N} = 2{,}5 * PRI_{p\,max} * M * N. \quad (5)$$

For Δf_{HF}= 80 MHz substituting the parameters $PRI_{p\,max} = 1000$ μs [21], $M = 6$ and $N = 6$ into Eq. (5), we obtain:

$$T_{scan} = T_f * \mathrm{N} = 2{,}5 * PRI_{p\,max} * M * N = 2{,}5 * 1000 * 10^{-6} * 6 * 6 = 0.09 \text{ s} \quad (6)$$

For Δf_{HF}= 500 MHz and $PRI_{p\,max} = 1000$ μs [21]:

$$T_{scan} = T_f * \mathrm{N} = 0.53 \text{ s} \quad (7)$$

The typical minimum aperture synthesis time T_{SAR} (excluding wide-area surveillance modes of spaceborne SARs) is 1 s or longer [22]. From Eqs. (6) and (7), a guaranteed search for emissions of airborne and spaceborne SARs is ensured, provided that the condition $T_{scan} < T_{SAR}$ is satisfied.

The algorithmic components were independently verified through computer simulations using synthetic SAR signals. These simulations confirmed both the accuracy of parameter estimation and the robustness of the Bayesian recognition module under low signal-to-noise ratio conditions. Collectively, these results demonstrate that the proposed

processing chain operates correctly at the algorithmic level and is suitable for real-time implementation in compact radiomonitoring systems.

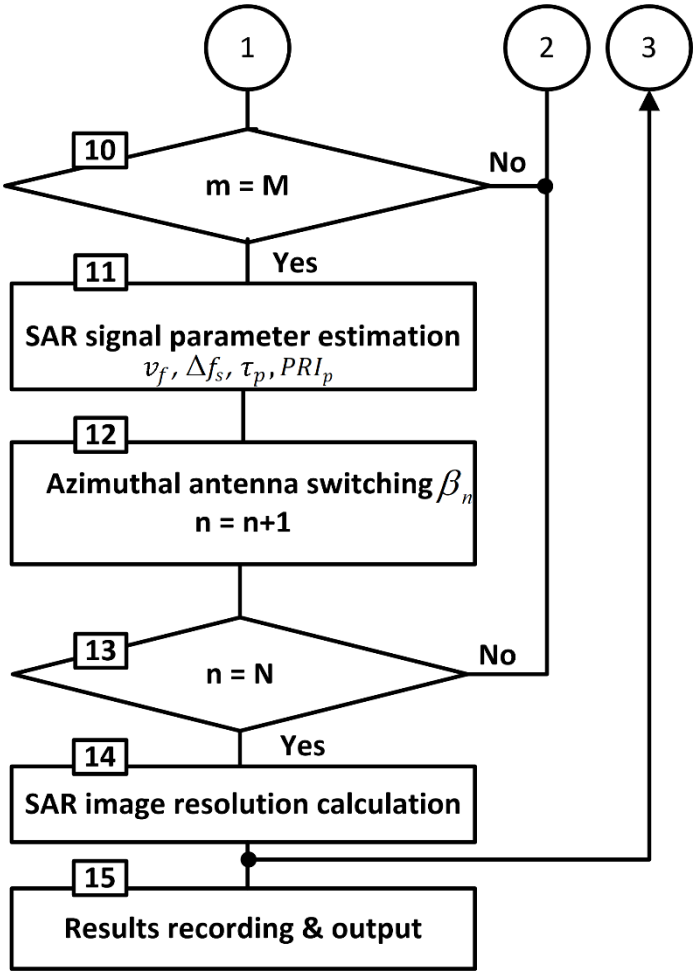

Fig. 8. Structural block diagram of the operating algorithm of the compact automatic SAR signal monitoring device (conclusion).

5. CONCLUSIONS

In this work, a compact automatic device for real-time radiomonitoring of SAR emissions has been developed. The proposed solution enables automatic detection of emission onset, classification of signals, analysis of technical parameters, and attribution of emissions to their respective sources. The simulation results demonstrate that the proposed processing scheme provides a parameter-estimation error below 8% and achieves classification probabilities approaching unity for representative SAR signal types at signal-to-noise ratios above 0 dB. These findings confirm the effectiveness of the developed algorithmic chain and its suitability for implementation in compact radiomonitoring modules.

Acknowledgement: The authors would like to thank the anonymous reviewers and editors for providing valuable suggestions and comments.

REFERENCES

[1] Z. Wang, Z. Zeng, G. Xu, Z. Xiong , S. Zhou, "UAV swarm SAR new Concept and fast time domain imaging algorithm, "2021 CIE International Conference on Radar, 2021, doi: 10.1109/Radar53847.2021.10028651.

[2] F. Brigui, S. Angelliaume, N. Castet, X. Dupuis, P. Martineau, "SAR-light - first SAR images from the new onera SAR sensor on UAV platform," IGARSS 2022 - 2022 IEEE International Geoscience and Remote Sensing Symposium, 2022, doi: 10.1109/IGARSS46834.2022.9884340.

[3] V. Vesely, C. Lee, T. Anand, U. Moon, "PLL-SAR: a new high-speed analog to digital converter architecture," 2023 IEEE 66th International Midwest Symposium on Circuits and Systems, 2023, doi: 10.1109/MWSCAS57524.2023.10405967.

[4] N. Nhan, A. Podstrigaev, T. Nghi, "A mathematical model for determining the type of signal modulation in a digital receiver with autocorrelation processing," 2021 IEEE Conference of Russian Young Researchers in Electrical and Electronic Engineering, 2021, doi: 10.1109/ElConRus51938.2021.9396097.

[5] N. Nhan, A. Podstrigaev, T. Nghi, "Estimation of the computational complexity of the algorithm for determining the type of signal modulation in the autocorrelation receiver," 2021 IEEE Conference of Russian Young Researchers in Electrical and Electronic Engineering, 2021, doi: 10.1109/ElConRus51938.2021.9396254.

[6] V. Likhachev, A. Podstrigaev, N. Nhan, V. Davydov, N. Myazin, "Study of the accuracy of determining the location of radio emission sources with complex signals when using autocorrelation and matrix receivers in broadband tools for analyzing the electronic environment," NEW2AN ruSMART 2020. Lecture Notes in Computer Science, 2020, doi: 10.1007/978-3-030-65726-0_29.

[7] N. Nhan, A. Podstrigaev, V. Likhachev, A. Veselkov, V. Davydov, N. Myazin, S. Makeev, "Study of detection characteristics in recognition of simple radio pulses and signals with LFM and PSK in the autocorrelation receiver," NEW2AN ruSMART 2020. Lecture Notes in Computer Science, 2020, doi: 10.1007/978-3-030-65726-0_37.

[8] J. Tsui, C. Cheng, *Digital Techniques for Wideband Receivers,* SciTech Publishing Inc., New York, United States, 2015.

[9] M. Skolnik, *Introduction to Radar Systems*, McGraw-Hill, New York, 2001.

[10] A. Rembovsky, A. Ashikhmin, V. Kozmin, S. Smolskiy, *Radio Monitoring: Problems, Methods, and Equipment*, Springer New York, NY, 2009.

[11] N. Nhan, D. M. Hoang, T. Nghi, "Analysis of the possibility of using an autocorrelation receiver in radio monitoring tools," *2024 Conference of Young Researchers in Electrical and Electronic Engineering*, 2024, doi: 10.1109/ElCon61730.2024.10468296.

[12] I. Islamov, *Modeling of Antenna and Waveguide Devices for Wireless and Satellite Communications Systems*, Springer Cham, 2025

[13] H. Visser, *Antenna Theory and Applications*, Wiley Telecom, 2012.

[14] C. Studer, S. Medjkouh, E. Gonultaş, T. Goldstein, O. Tirkkonen, "Channel charting: locating users within the radio environment using channel state information," *IEEE Access*, vol. 6, pp. 47682-47698, 2018, doi: 10.1109/ACCESS.2018.2866979.

[15] P. Kyösti, P. Zhang, A. Pärssinen, K. Haneda, P. Koivumäki, W. Fan, "On the feasibility of out-of-band spatial channel information for millimeter-wave beam search," *IEEE Transactions on Antennas and Propagation*, vol. 71, no. 5, pp. 4433-4443, 2023, doi: 10.1109/TAP.2023.3249837.

[16] R. Warty, M. Tofighi, U. Kawoos, A. Rosen, "Characterization of implantable antennas for intracranial pressure monitoring: reflection by and transmission through a scalp phantom," *IEEE Transactions on Microwave Theory and Techniques*, vol. 56, no. 10, pp. 2366–2376, 2008, doi: 10.1109/TMTT.2008.2004254.

[17] L. García, G. Furano, M. Ghiglione, V. Zancan, E. Imbembo, C. Ilioudis, "Advancements in onboard processing of synthetic aperture radar (SAR) data: enhancing efficiency and real-time capabilities, " *IEEE Journal of Selected Topics in Applied Earth Observations and Remote Sensing*, vol. 17, pp. 16625-16645, 2024, doi: 10.1109/JSTARS.2024.3406155.

[18] Y. Li, A. Guarnieri, C. Hu, F. Rocca, "Performance and requirements of GEO SAR systems in the presence of radio frequency interferences," *Remote Sensing*, vol. 10, no. 1, p. 82, 2018, doi: 10.3390/rs10010082.

[19] W. Meng, Z. Cai, F. Fang, D. Feng, J. Wang, S. Xing, S. Quan, "Detection and type recognition of SAR artificial modulation targets based on multi-scale amplitude-phase features," *Remote Sensors*, vol. 16, p. 2107, 2024, doi: 10.3390/rs16122107.

[20] S. Huan, G. Dai, G. Luo, S. Ai, "Bayesian compress sensing based countermeasure scheme against the interrupted sampling repeater jamming," *Sensors (Basel)*, vol. 15, p. 3279, 2019, doi: 10.3390/s19153279. PMID: 31349709.

[21] M. Rysz, A. Tsokas, K. Dipple, K. Fair, P. Pardalos, *Synthetic Aperture Radar (SAR) Data Applications*, Springer Cham, 2022.

[22] K. Chen, *Radar Scattering and Imaging of Rough Surfaces*, CRC Press, 2020.